



Universiteit
Leiden
The Netherlands

Structure and Function of the Left Atrium and Left Atrial Appendage AF and Stroke Implications

Delgado, V.; Biase, L. di; Leung, M.; Romero, J.; Tops, L.F.; Casadei, B.; ... ; Bax, J.J.

Citation

Delgado, V., Biase, L. di, Leung, M., Romero, J., Tops, L. F., Casadei, B., ... Bax, J. J. (2017). Structure and Function of the Left Atrium and Left Atrial Appendage AF and Stroke Implications. *Journal Of The American College Of Cardiology*, 70(25), 3157-3172. doi:10.1016/j.jacc.2017.10.063

Version: Not Applicable (or Unknown)
License: [Leiden University Non-exclusive license](#)
Downloaded from: <https://hdl.handle.net/1887/95001>

Note: To cite this publication please use the final published version (if applicable).

REVIEW TOPIC OF THE WEEK

Structure and Function of the Left Atrium and Left Atrial Appendage



AF and Stroke Implications

Victoria Delgado, MD, PhD,^a Luigi Di Biase, MD, PhD,^b Melissa Leung, MBBS, BSc(MED), MBIostat, PhD,^c Jorge Romero, MD,^b Laurens F. Tops, MD, PhD,^a Barbara Casadei, MD, PhD,^d Nassir Marrouche, MD, PhD,^e Jeroen J. Bax, MD, PhD^a

ABSTRACT

Atrial fibrillation (AF) and stroke are important major health problems that share common risk factors and frequently coexist. Left atrial (LA) remodeling is an important underlying substrate for AF and stroke. LA dilation and dysfunction form a prothrombotic milieu characterized by blood stasis and endothelial dysfunction. In addition, alterations of the atrial cardiomyocytes, increase of noncollagen deposits in the interstitial space and fibrosis, favor the occurrence of re-entry that predisposes to AF. Eventually, AF further impairs LA function and promotes LA remodeling, closing a self-perpetuating vicious circle. Multimodality imaging provides a comprehensive evaluation of several aspects of LA remodeling and offers several parameters to identify patients at risk of AF and stroke. How multimodality imaging can be integrated in clinical management of patients at risk of AF and stroke is the focus of the present review paper. (J Am Coll Cardiol 2017;70:3157-72) © 2017 by the American College of Cardiology Foundation.

Atrial fibrillation (AF) and stroke are highly prevalent conditions that share common risk factors and frequently coexist (1). The presence of AF is independently associated with 5-fold increased risk of stroke (2,3). Left atrial (LA) remodeling is an important underlying substrate for AF and stroke. Data from a population-based cohort showed that LA dilation provided good accuracy to identify the individuals that will present with AF

(area under the curve 0.86) (4). In addition, a recent systematic review including 67,875 participants in sinus rhythm demonstrated that the risk of stroke increases along with the LA size (5). Age, obesity, diabetes mellitus, hypertension, and sleep apnea cause LA dilation and dysfunction, creating a prothrombotic milieu characterized by blood stasis and endothelial dysfunction. This type of atrial cardiomyopathy has been suggested as a cause of



Listen to this manuscript's
audio summary by
JACC Editor-in-Chief
Dr. Valentin Fuster.



From the ^aDepartment of Cardiology, Leiden University Medical Center, Leiden, the Netherlands; ^bDivision of Cardiology, Section of Cardiac Electrophysiology, Montefiore Medical Center, Albert Einstein College of Medicine, New York, New York; ^cDepartment of Cardiology, Liverpool Hospital, University of New South Wales, Sydney, New South Wales, Australia; ^dRadcliffe Department of Medicine, Division of Cardiovascular Medicine, University of Oxford, Oxford, United Kingdom; and the ^eDivision of Cardiology, Section of Cardiac Electrophysiology, University of Utah Health Sciences Center, Salt Lake City, Utah. The Department of Cardiology of the Leiden University Medical Center has received unrestricted research grants from Medtronic, Biotronik, Boston Scientific, and Edwards Lifesciences. Dr. Delgado has received speaker fees from Abbott Vascular. Dr. Di Biase is a consultant for Stereotaxis, Biosense Webster, and St. Jude Medical; and has received honoraria/travel fees from Medtronic, Biotronik, Boston Scientific, EpiEP, Pfizer, and Janssen. Dr. Leung has received grants from Pfizer. Dr. Casadei has received measurements of blood-based biomarkers by Roche Diagnostics at no cost to the investigators. Dr. Marrouche has been a consultant for Abbott, Biotronik, Cardiac Design, Medtronic, Preventice, Vytronus, Biosense Webster, Marrek, and Boston Scientific; has received research funding from Abbott, Boston Scientific, GE Healthcare, Siemens, Biotronik, Bytronus, and Biosense Webster; and has company interest in Marrek and Cardiac Design. All other authors have reported that they have no relationships relevant to the contents of this paper to disclose.

Manuscript received October 1, 2017; accepted October 22, 2017.

ABBREVIATIONS AND ACRONYMS

2D = 2-dimensional

3D = 3-dimensional

AF = atrial fibrillation

CMR = cardiovascular magnetic resonance

CT = computed tomography

IQR = interquartile range

LA = left atrial/atrium

LAA = left atrial appendage

LGE = late gadolinium enhancement

LV = left ventricle/ventricular

PA-TDI = P-wave to peak A'-wave on tissue Doppler imaging

TDI = tissue Doppler imaging

TEE = transesophageal echocardiography

thromboembolism before AF occurs. In addition, LA remodeling is accompanied by alterations of the atrial cardiomyocytes, increase of noncollagen deposits in the interstitial space, and fibrosis that favor the occurrence of re-entry that predisposes to AF. AF subsequently further impairs LA function and promotes LA remodeling.

Currently, risk stratification of AF patients for the occurrence of stroke is based on clinical scores that do not include LA remodeling and function in their algorithms. By contrast, novel therapeutic options such as radiofrequency catheter ablation techniques and transcatheter closure of the left atrial appendage (LAA) demand advanced imaging to maximize patient safety and procedural outcomes. Multimodality imaging provides a comprehensive evaluation of several aspects of LA remodeling and offers several parameters to identify patients at risk

of AF and stroke. The present review paper summarizes the role of multimodality imaging to assess the pathophysiology of AF and stroke, and highlights the key parameters to answer specific clinical questions. 1) What are the LA and LAA remodeling characteristics associated with AF and stroke? 2) How can imaging help to identify the patients who will benefit from invasive therapies (AF ablation and LAA closure)?

LA: NORMAL ANATOMY AND FUNCTION

Because LA structural remodeling and AF are closely related, it is recommended that LA size and anatomy be assessed routinely in all AF patients (6). LA size is typically assessed with standard 2-dimensional (2D) echocardiography. The LA anteroposterior diameter derived from a conventional parasternal long-axis view is used to estimate LA size. However, because asymmetrical remodeling occurs in LA dilation, it is recommended that LA volumes be assessed using a volumetric method, such as the modified Simpson biplane method of discs (Figure 1). With the use of 3-dimensional (3D) imaging modalities, LA volumes can be assessed even more accurately. Real-time 3D echocardiographic measurements of LA volumes have been validated against computed tomography (CT) and cardiovascular magnetic resonance (CMR), and the technique has improved diagnostic accuracy and reproducibility compared with 2D echocardiography (Figure 1). Normal reference values for 3D LA volume are 15 to 42 ml/m² in men and 15 to 39 ml/m² in women (7). Furthermore, assessment of pulmonary

vein anatomy is relevant when an ablation procedure is considered in AF patients. It has been demonstrated that pulmonary vein anatomy is highly variable. Variations in the number and location of the pulmonary veins are associated with outcome in catheter ablation procedures for AF (8). Typically, CT or CMR is performed before the ablation procedure to assess pulmonary vein anatomy. The 3D reconstructed images provide detailed information on LA and pulmonary vein anatomy that can be used to guide the ablation procedure.

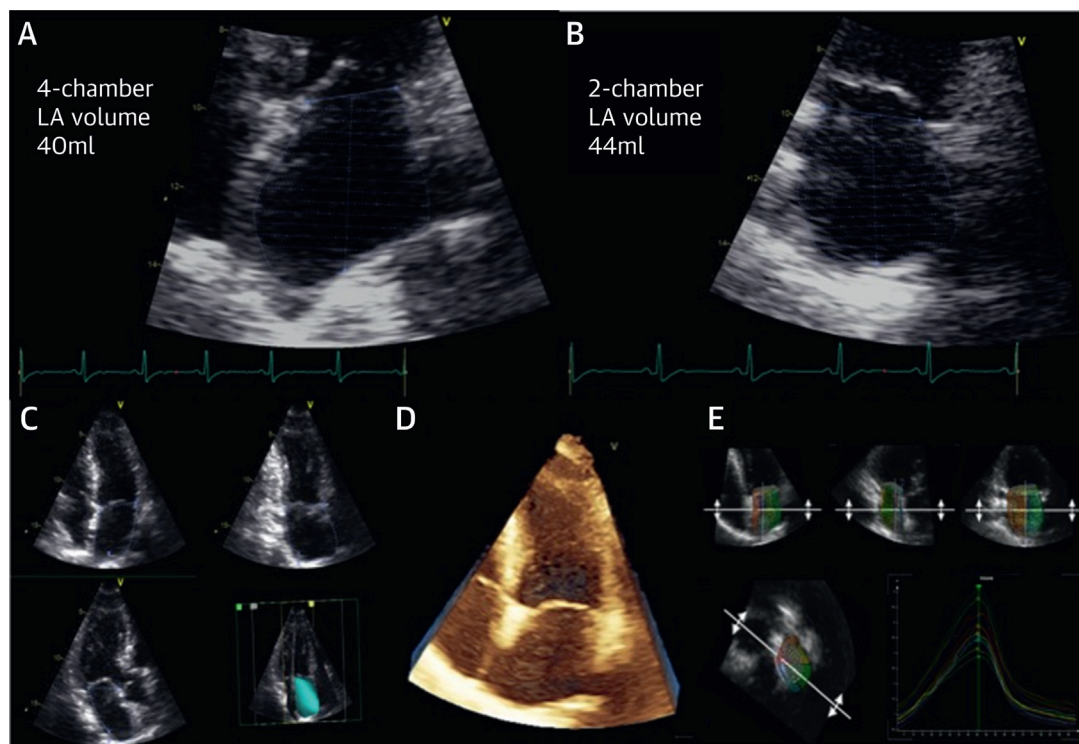
In addition to the anatomic information of the LA, assessment of LA function is important because it contributes 30% of the left ventricular (LV) stroke volume. Impaired LA function has been associated with increased risk of stroke and AF (5,9). Normal LA function can be divided into 3 distinct phases. During ventricular systole, the LA serves as a reservoir for blood drained by the pulmonary veins. During early ventricular diastole, the LA is a conduit for the pulmonary venous return. During late systole, the booster pump function of the LA completes the LV filling. Whereas the LA reservoir function is determined by atrial compliance, atrial relaxation, and contractility, as well as LV systolic function and end-systolic volume, the LA conduit function is influenced by LA compliance and LV relaxation and compliance, and the LA booster pump function is influenced by venous return, LV end-diastolic pressures, and systolic reserve. These 3 functions can be assessed with echocardiographic and CMR techniques. How anatomic and functional assessment of the LA permits stratification of patients with AF is discussed in the next sections.

LA REMODELING: SUBSTRATE FOR AF

LA dilation and myocardial fibrosis causing LA dysfunction and electromechanical conduction delay characterize LA remodeling and form the substrate for AF. In recent years, there has been a resurgence of interest in imaging the LA to better understand the LA structural and functional changes associated with new-onset and perpetuation of AF. LA volumes preferably assessed with 3D imaging techniques are frequently considered in the therapeutic decision making of AF patients. LA volume has been shown to be a stronger determinant of success of radiofrequency catheter ablation techniques than the type of AF (i.e., paroxysmal vs. persistent) (10).

Late gadolinium contrast enhanced (LGE) CMR has significantly improved our understanding of atrial fibrosis as the hallmark of structural LA remodeling in AF. Gadolinium contrast media accumulate in the

FIGURE 1 LA Volume Assessment Using 2D and 3D Echocardiography

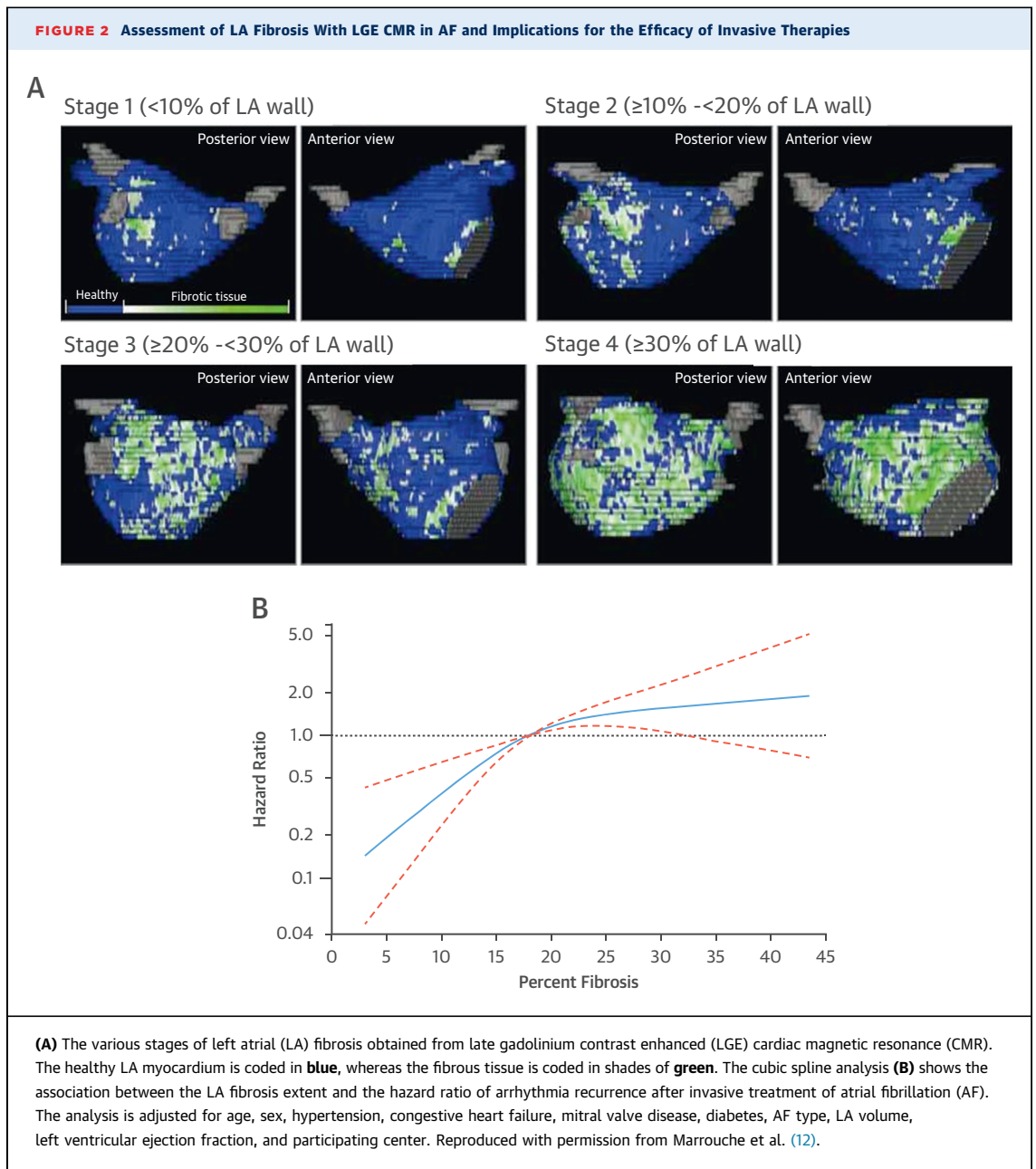


(A and B) The 2-dimensional (2D) echocardiographic measurement of left atrial (LA) volume using the Simpson biplane approach in the apical 4-chamber **(A)** and 2-chamber **(B)** views are shown. The LA appendage is not included in the tracing of the endocardial border. **(C)** Real-time 3-dimensional (3D) echocardiographic measurement of LA volumes is shown. LA volumes may be obtained with improved anatomic alignment, by tracing the blood tissue interface on 3D-guided triplane images in the apical 4-, 2-, and 3-chamber views **(C)**. Live-3D **(D)** and full-volume multibeam reconstructions **(E)** may also be used to measure LA volumes at any phase of the cardiac cycle, providing improved alignment at the geometric center of the left atrium.

extracellular space and appear as bright white areas in the atrial myocardium. A dynamic threshold algorithm identifies the regions of fibrosis as areas with thresholds 2 to 4 SD higher than the threshold defining normal LA myocardial tissue (11). On the basis of the extent of LA LGE, a classification of LA fibrosis has been proposed ranging from stage 1, when the fibrosis extension is <10% of the LA wall, to stage 4 when the extension of fibrosis is $\geq 30\%$ (Figure 2) (12). The presence of interstitial fibrosis in the subepicardial myocardium favors electrical dissociation and leads to wave breaks and rotors that characterize AF (13,14). LA fibrosis extent has been shown to significantly impact on the efficacy of radiofrequency catheter ablation techniques for AF (12). The DECAAF (Delayed-Enhancement Magnetic Resonance Imaging Determinant of Successful Radiofrequency Catheter Ablation of Atrial Fibrillation) study provides evidence that the

pre-ablation fibrosis burden should be taken into consideration when selecting patients for catheter ablation (12). Each 1% increase in LA fibrosis was independently associated with 6% increased risk of arrhythmia recurrence at follow-up. Patients with <20% LA fibrosis (stages 1 and 2) had the lower hazards of presenting with arrhythmia recurrence after catheter ablation (Figure 2).

Assessment of LA function provides further insights in the consequences of LA structural remodeling. The association between LA reservoir function and AF has been shown in 574 adults without arrhythmia followed up for a mean of 1.9 ± 1.2 years (15). The age-adjusted risk of AF or atrial flutter was highest for subjects with both reduced LA reservoir function (<49%) and increased maximum LA volume (>38 ml/m²). Advanced echocardiographic techniques such as pulsed-wave or color-coded tissue Doppler imaging (TDI) enable assessment of the peak

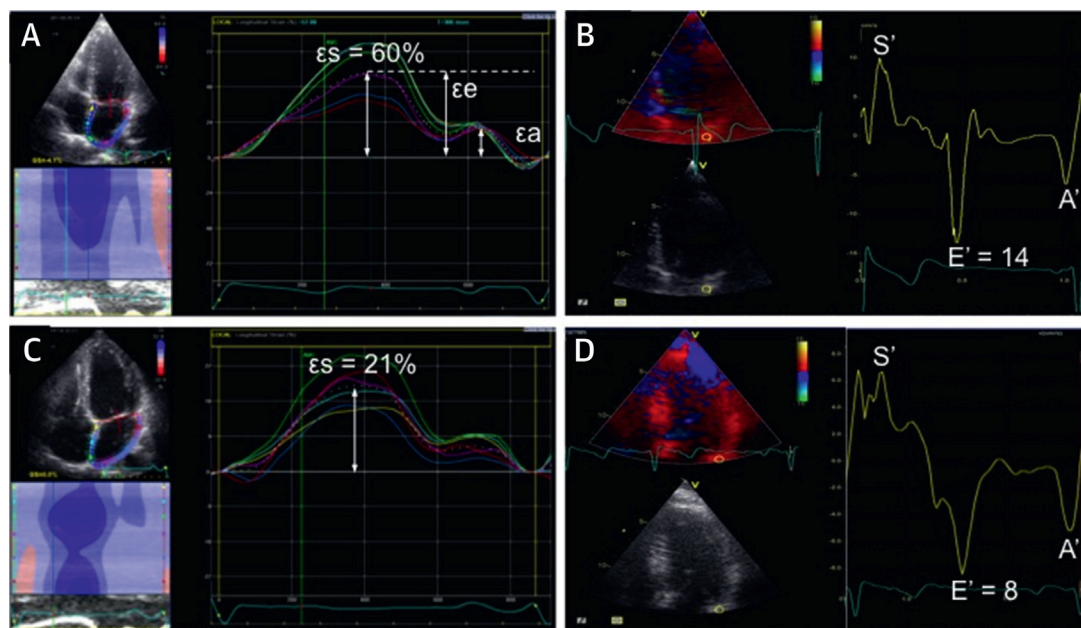


velocity at the mitral annulus in late diastole due to atrial contraction (A') (**Figure 3**). In patients with chronic AF cardioverted to sinus rhythm, low segmental atrial velocities have been demonstrated immediately post-cardioversion followed by a temporal increase in segmental atrial contractility up to 6 months later (16). In addition, strain and strain rate imaging examine the magnitude and the rate of myocardial deformation during the cardiac cycle and may be assessed using either color-coded TDI or 2D speckle tracking or vector velocity imaging (**Figure 3**).

A reduced LA reservoir strain has been shown to correlate with LA wall fibrosis on CMR in patients with AF (11). In patients undergoing catheter ablation for AF, LA reservoir function is predictive of maintaining sinus rhythm (17), and is an independent predictor of LA reverse remodeling (18).

The LA remodeling process has been also associated with electrical remodeling with areas of slow conduction, shortening of the atrial refractoriness, and increased nonuniform anisotropy that lead to re-entrant circuits and AF. Surface electrocardiograms,

FIGURE 3 LA Function Assessment Using Strain Measured by 2D Speckle Tracking Echocardiography and Color-Coded TDI Velocities



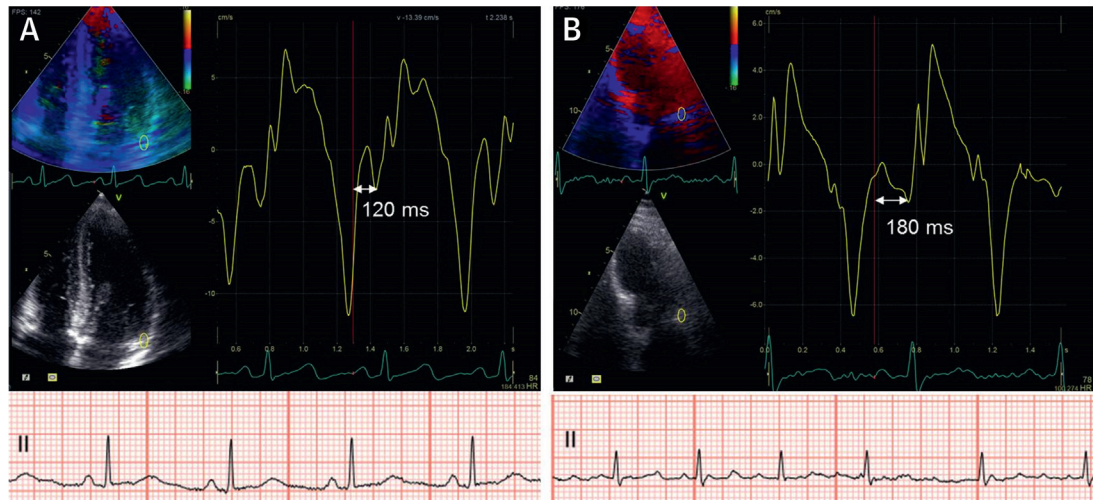
(A and C) The peak positive longitudinal strain (ϵ_s), corresponding to atrial reservoir function, the strain during early and late diastole (ϵ_e and ϵ_a , respectively) corresponding to the conduit and booster pump function, with left ventricular end-diastole (QRS onset) as the reference point are shown. The atrial color-coded tissue Doppler imaging (TDI) velocity trace obtained with the sample volume placed in the basal lateral atrial wall is shown in **B and D**. The trace represents the atrial velocities measured in this region throughout the cardiac cycle. The S' is positive and occurs in ventricular systole; the E' and A' are negative deflections and occur in early and late ventricular diastole, respectively. **A** shows a normal subject with preserved peak left atrial (LA) strain of 60%. This same patient has a normal E' velocity of 14 cm/s (**B**). **C** displays a patient with history of paroxysmal atrial fibrillation and reduced peak LA strain of 21%, and E' velocity of 8 cm/s (**D**).

conventional endocardial electrograms, or 3D electroanatomic mapping systems characterize the electrical remodeling. Color-coded TDI echocardiography by way of P-wave to peak A'-wave on TDI (PA-TDI), provides a noninvasive parameter reflecting the electromechanical delay, likely reflecting fibrosis formation in the LA (**Figure 4**). More specifically, PA-TDI is the time delay between the electrical LA activation (indicated by the P-wave on the surface electrocardiogram) and the mechanical atrial contraction (reflected by the peak A'-wave on TDI). The value of PA-TDI to predict new-onset AF was evaluated in 249 patients without previous AF (19). Patients who presented with AF ($n = 15$, 6%) during follow-up had longer PA-TDI duration than patients who remained in sinus rhythm (172 ± 25 ms vs. 150 ± 20 ms; $p = 0.001$). Prolonged PA-TDI was independently associated with new-onset AF (odds ratio: 1.37; $p = 0.027$). This parameter has also been correlated with the efficacy of radio-frequency catheter ablation: patients with longer

PA-TDI had higher risk of AF recurrences at follow-up (odds ratio: 1.04; $p < 0.001$) (20).

Finally, imaging of the adipose tissue that accumulates around the LA provides additional insights in the pathophysiology of AF. Fatty tissue infiltrating the atrial subepicardium is universally observed (13). However, in patients with AF, the fatty tissue shows characteristic structural remodeling with adipocytes intermingling with fibrous bundles, myocytes, and thick and irregular epicardium. The extent of fibrosis within this fatty infiltration is significantly larger among patients with persistent AF ($64 \pm 23\%$) as compared with paroxysmal AF and sinus rhythm patients ($50 \pm 21\%$ vs. $37 \pm 24\%$, respectively; $p = 0.0004$) (13). Studies using CT have correlated the extent of adipose LA tissue with the presence of AF (21-23). In a recent study including 400 patients evaluated with CT, each gram increase of posterior LA adipose tissue was associated with 1.32 odds ratio of having AF (95% confidence interval: 1.22 to 1.43; $p < 0.001$) (23).

FIGURE 4 Measurement of the Time Delay Between Electrical and Mechanical Activation of the LA (PA-TDI) and Its Association With AF Ablation Efficacy



From the onset of the electrical activation of the left atrium (P-wave on surface electrocardiogram [red line]), the time to peak myocardial velocity of the LA contraction is measured (P-wave to peak A'-wave on tissue Doppler imaging [PA-TDI]). In **A**, the patient had a PA-TDI of 120 ms and remained in sinus rhythm after AF ablation. By contrast, the patient presented in **B** had longer PA-TDI (180 ms) and presented with recurrence of AF after ablation. Abbreviations as in [Figures 1 to 3](#).

LA AND RISK FOR STROKE

Cardioembolic stroke secondary to AF accounts for 15% of all ischemic strokes (24). Current risk scoring systems to estimate the risk of stroke in patients with AF and to identify those who will benefit from anticoagulation therapy are primarily based on demographic and clinical characteristics. However, the accuracy of these risk score systems to predict ischemic stroke in AF patients is modest, which may lead to overuse of anticoagulation in low-risk patients (25,26).

Several cardiac imaging-based variables have been associated with increased risk of stroke in AF patients ([Table 1](#)) (27). However, it remains unclear whether the addition of those variables to current risk scoring systems would lead to superior stroke risk stratification. The LA remodeling process associated with AF forms a milieu that enhances the risk of blood stagnation and thrombus formation. Several studies have shown that increased LA dimensions, presence of spontaneous echo contrast (sludge), and LAA thrombus and LAA flow peak velocity <20 cm/s measured on echocardiography, and LAA non-chicken wing morphology as assessed on multidetector row CT and CMR are associated with increased risk of stroke in AF patients (28-30). In addition, LA reservoir function measured with 2D

speckle tracking longitudinal strain echocardiography has also been associated with increased risk of stroke (9). In a case-control study, Leong et al. (9) showed that LA reservoir function was significantly lower in patients with stroke as compared with controls ($30 \pm 7.3\%$ vs. $34 \pm 6.7\%$; $p < 0.001$). Each 1% reduction in LA reservoir function was associated with 7% increase in the risk of stroke ($p < 0.001$). Using tissue-tracking

TABLE 1 LA and LAA Imaging-Based Variables to Predict Stroke

| | |
|---------------------------------------|--|
| Conventional echocardiography | LA dilation (M-mode) |
| | Spontaneous echo contrast |
| | LAA thrombus |
| | LAA peak velocity <20 cm/s (pulsed-wave Doppler) |
| Speckle tracking echocardiography | LAA non-chicken wing shape |
| | LA longitudinal strain (reservoir function) |
| Cardiac magnetic resonance | LA volume |
| | LA longitudinal strain (reservoir function, tissue tracking CMR) |
| | LA fibrosis (LGE-CMR) |
| | LA flow (4D-CMR) |
| | LAA non-chicken wing shape |
| Multidetector row computed tomography | LAA non-chicken wing shape |

4D = 4-dimensional; CMR = cardiac magnetic resonance; LA = left atrium; LAA = left atrial appendage; LGE = late gadolinium enhancement.

CMR, Inoue *et al.* (31) demonstrated larger LA volumes and lower LA longitudinal strain on tissue-tracking CMR (reflecting more impaired LA reservoir function) among patients with AF and history of stroke or transient ischemic attack. LA reservoir function was independently associated with stroke (odds ratio: 0.91; $p = 0.018$) and had incremental diagnostic value over CHA₂DS₂VASc score and LA volume. In addition, the extent of LA fibrosis on LGE-CMR has been associated with the presence of spontaneous echo contrast and LAA thrombus (32). Patients with AF and extensive LA fibrosis (>20%) were more likely to show spontaneous echo contrast (odds ratio: 2.6; $p = 0.06$) and LAA thrombus (odds ratio: 4.6; $p = 0.02$). Daccarett *et al.* (33) demonstrated the independent association between LA fibrosis and stroke in 387 AF patients. Patients with history of stroke ($n = 36$, 9.3%) showed significantly more LA fibrosis as compared with patients without stroke ($24.4 \pm 12.4\%$ vs. $16.2 \pm 9.9\%$, respectively; $p < 0.001$). The addition of LA fibrosis extent to a model including the clinical predictors of stroke (congestive heart failure, age >75 years, diabetes mellitus, and hypertension) improved the predictive statistics (shifting the area under the curve from 0.58 to 0.72).

These structural and functional LA changes may lead to reduced LA flow dynamics and blood stagnation. Four-dimensional (4D) flow CMR permits assessment of blood flow patterns over time in the LA (Figure 5) (34). With this imaging technique, it has been shown that patients with AF exhibit 8% to 26% reduction in mean, median, and peak LA flow velocities as compared with age-matched controls (34). However, the incremental predictive value of LA flow velocities measured with 4D flow CMR over current risk score models has not been evaluated.

Future studies prospectively evaluating the predictive value of LA and LAA imaging-based variables for stroke in AF patients will establish the role of these parameters to identify the patients who will benefit from anticoagulation therapy.

LAA ANATOMY AND FUNCTION: IMPLICATIONS FOR STROKE AND THERAPY

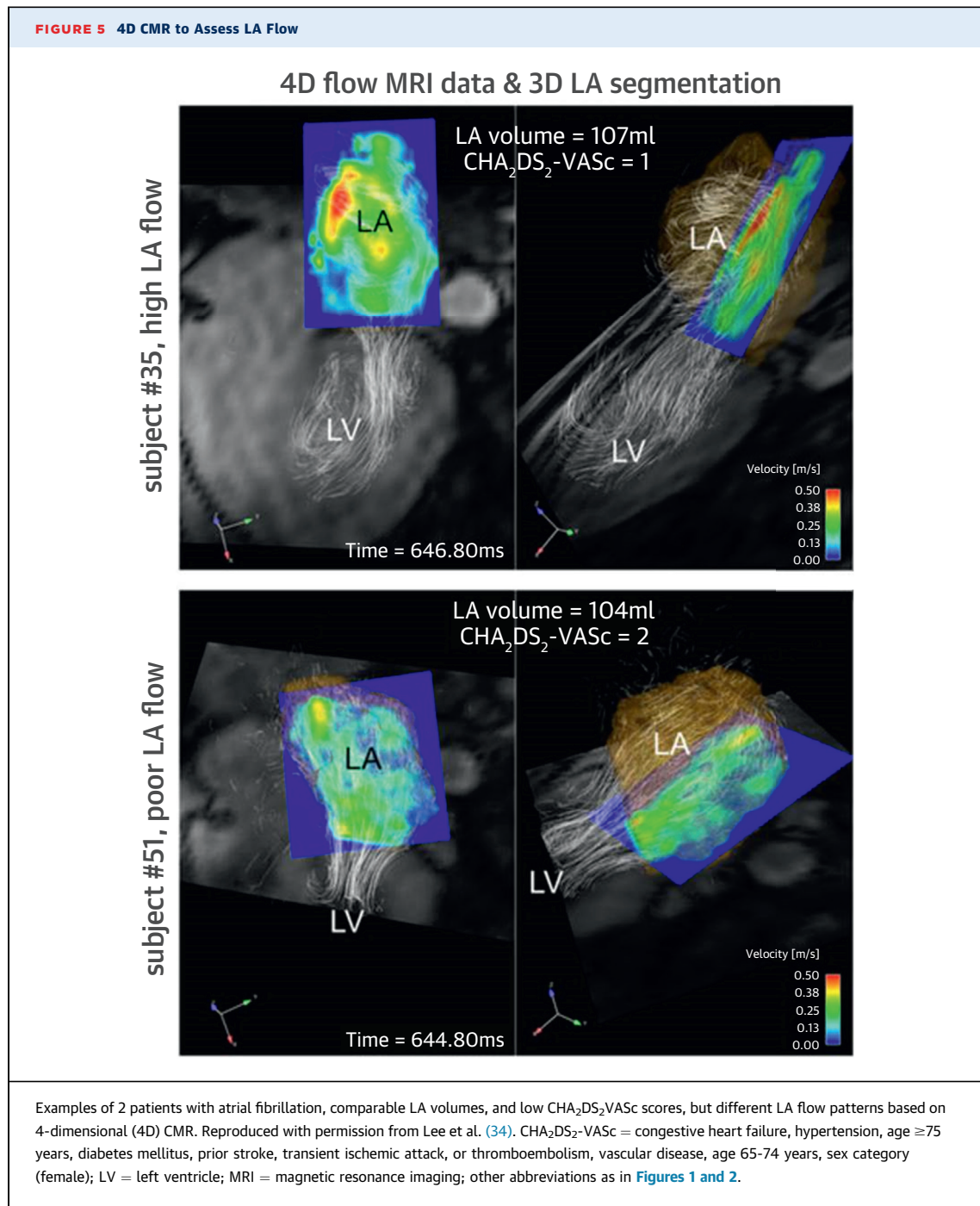
The LAA is a finger- or stump-like extension of the LA with lobes that may harbor up to 90% of thrombi that occur in patients with AF (35). In contrast to the smooth-walled LA, the LAA contains pectinate muscles that form a complex network of muscular ridges. The transition between the rough endocardium of the LAA to the smooth-walled LA is demarcated by the ostium of the LAA, well defined posteriorly by the ridge that separates the superior left pulmonary vein.

The shape of the LAA is largely variable and can be classified based on the shape and number of lobes (Figure 6) (36). Important anatomic relationships of the LAA to take into account when planning transcatheter closure and radiofrequency ablation of this structure include the superior left pulmonary vein, the mitral valve, and the circumflex coronary artery (Figure 7) (37). The LAA also has important mechanical and endocrinological functions (38): the LAA has contractile properties, and its distensibility is larger than the LA, contributing to LA pressure modulation (39). In addition, the concentration of atrial natriuretic peptide is largest in the LAA (40). Through activation of stretch-sensitive receptors and the effects of the atrial natriuretic peptide on heart rate, diuresis, and natriuresis, the LAA helps to modulate the LA pressure (38).

The LAA is also an important source of AF (41). Of 987 patients undergoing radiofrequency catheter ablation, 27% showed firing from the LAA, whereas in 8.7%, the LAA was the only source of arrhythmia. The BELIEF (Effect of Empirical Left Atrial Appendage Isolation on Long-Term Procedure Outcome in Patients With Longstanding Persistent Atrial Fibrillation Undergoing Catheter Ablation) study showed that the addition of electrical LAA isolation to extensive ablation of the LA resulted in lower rates of AF recurrence at 12-month follow-up, as compared with extensive ablation of the LA alone (44% vs. 72%) (42).

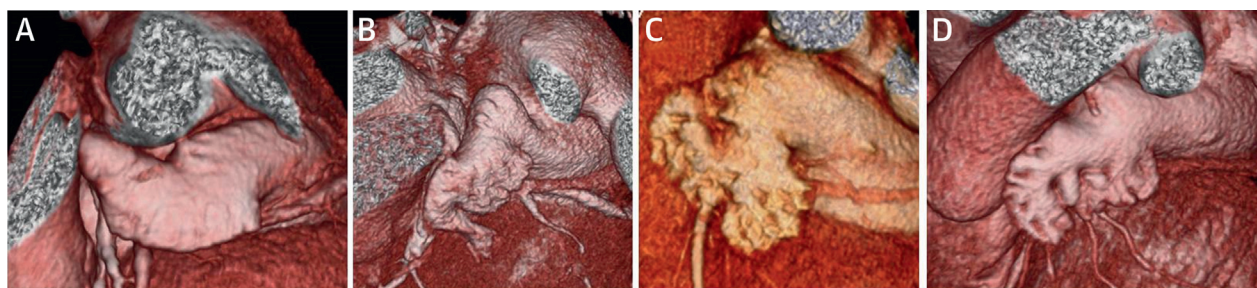
Echocardiography is the imaging technique of first choice to evaluate the LAA. Particularly, transesophageal echocardiography (TEE) permits accurate assessment of the LAA anatomy and is the reference standard to diagnose thrombus (sensitivity 100% and specificity 99%) (43). The presence of dense spontaneous echo contrast and large dimensions of the LAA (>34 cm³) have been associated with increased risk of stroke (28,44,45). The use of ultrasound contrast agents during TEE improve the diagnostic accuracy for LAA thrombus and reduces the number of uncertain results from 17.8% to 5.6% (46). The function of the LAA is most commonly assessed with pulsed-wave Doppler tracing of the LAA flow. In AF, the LAA flow pattern is characterized by saw tooth signals of variable amplitude (Figure 8). LAA systolic velocities <20 cm/s have been associated with spontaneous echo contrast and risk of stroke (47).

3D imaging techniques such as 3D TEE, CMR, and CT provide accurate measurements of the LAA appendage size, visualization of LAA thrombus, and assessment of the anatomic spatial relationships to be considered for transcatheter LAA closure. 3D TEE is key during the planning and guidance of



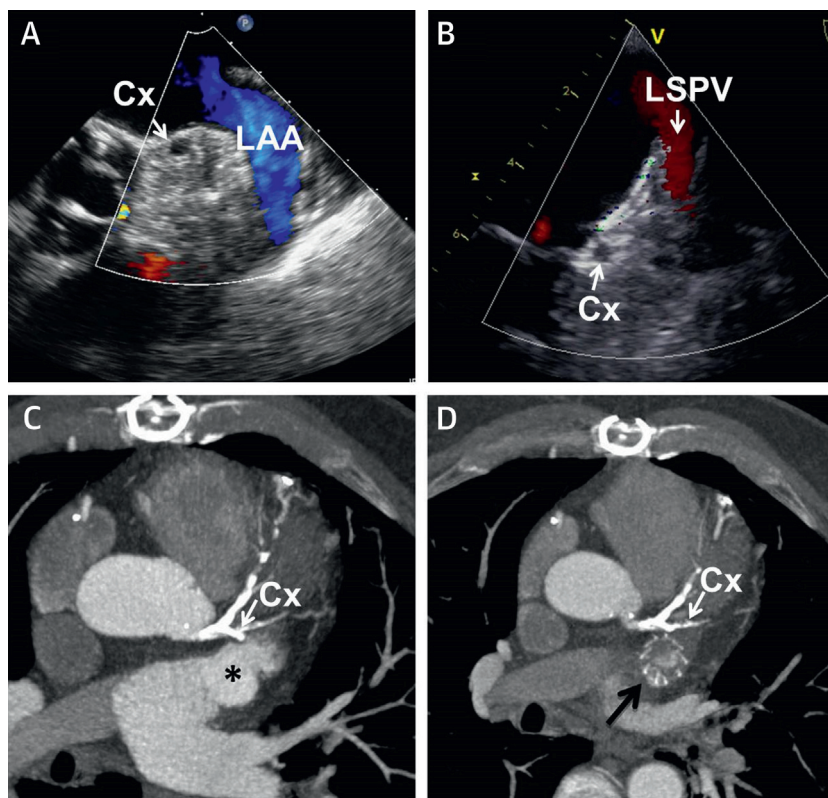
transcatheter LAA closure. By aligning the multiplanar reformation planes, the dimensions of the ostium and the landing zone where the closure device will be deployed can be measured ([Figure 9](#)). However, the morphology of the LAA is better visualized with multidetector row CT. A recent meta-analysis including 8 studies and 2,596 patients with AF (84% with CHADS₂ score) showed that chicken wing LAA morphology was associated with lower risk of thromboembolic event as compared with other morphologies (odds ratio: 0.46; 95% confidence interval: 0.36 to 0.58) ([48](#)). For detection of LAA thrombus, multidetector row CT data should be acquired with specific protocols that ensure full replenishment of the LAA by iodinated contrast ([49-51](#)). Furthermore, CT provides comprehensive information for selection of LAA closure device in AF patients with relative or absolute contraindications

FIGURE 6 Morphology of the LAA



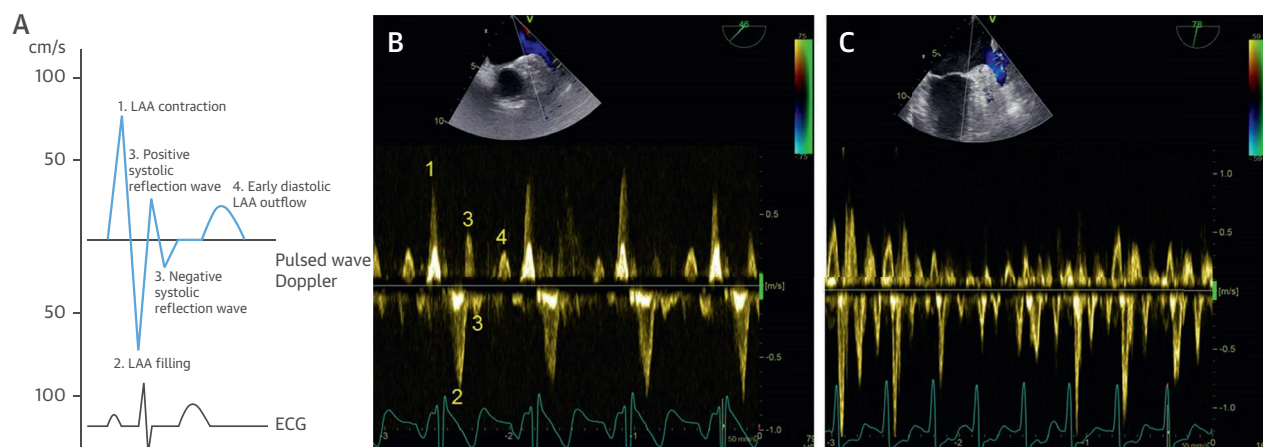
The classification of the left atrial appendage (LAA) morphology is based on the shape of the central and secondary lobes: windsock (**A**) (with 1 central lobe), chicken wing (**B**) (with a central lobe bended), cauliflower (**C**) (when the central lobe is short and with several lobes leading to a distal width larger than the proximal part), and cactus (**D**) (with a central lobe leading to several secondary lobes superior and inferiorly).

FIGURE 7 Anatomic Relationships of the LAA to Consider in Transcatheter Closure Procedures



Example of a patient receiving an AMULET device closure (**A and B**). Note the anterior position of the circumflex coronary artery (Cx) relative to the left atrial appendage (LAA) at baseline (**A**). After insertion of the device, the Cx is patent, and the flow of the left superior pulmonary vein (LSPV) is not compromised (**B**). In **C and D**, an example of a patient receiving a WATCHMAN device is shown. The anterior spatial relationship of the Cx and the LAA (asterisk) can be analyzed with computed tomography (**C**). Note the close proximity of the deployed device to the Cx (black arrow) (**D**). Reprinted with permission from Ismail et al. (37).

FIGURE 8 Assessment of LAA Function

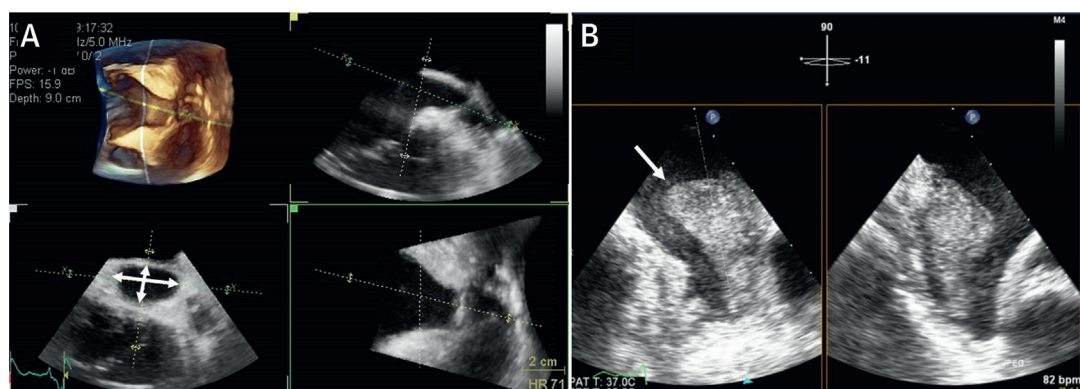


(A) A schematic pulsed-wave Doppler recording of the left atrial appendage (LAA) flow velocities across the cardiac cycle (electrocardiogram). **(B)** The pulsed-wave Doppler recording of a patient in sinus rhythm is displayed. Note that the **numbers** correspond to the wave reflections during LAA contraction, LAA filling, late systolic reflections, and early diastolic LAA outflow as in the schematic representation of **A**. During atrial fibrillation, the pulsed-wave Doppler pattern of the LAA flow resembles a saw tooth **(C)**.

for oral anticoagulation. Currently available devices differ in size, shape, and methodology of deployment: whereas the Amplatzer AMULET (St. Jude Medical, Plymouth, Massachusetts) consists of a self-expandable nitinol distal lobe anchored in the neck of the LAA and a proximal disc that enhances the complete closure of the ostium, the WATCHMAN device (Boston Scientific, Natick, Massachusetts) is a nitinol cage with 10 peripheral anchors and a fabric



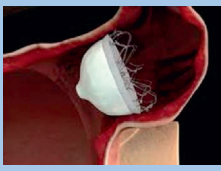
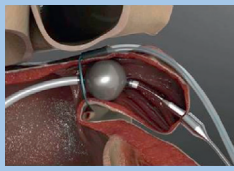
cap that is anchored in the ostium of the LAA. The LARIAT device (SentreHEART, Redwood City, California), by contrast, is a combined endocardial and epicardial method to exclude the LAA. The anatomic prerequisites for each device are well defined by the manufacturers (**Figure 10**). The evidence from a limited number of randomized trials has demonstrated that transcatheter LAA closure is noninferior to warfarin in AF patients (**52**).

FIGURE 9 Assessment of LAA Dimensions and Evaluation of Thrombus Before Transcatheter Closure



(A) The multiplanar reformation planes from 3-dimensional transesophageal echocardiography volume acquisition. The planes are aligned to obtain the cross-sectional view of the left atrial appendage (LAA) ostium. The presence of large thrombus is a contraindication for transcatheter closure of the LAA **(B, arrow)**.

FIGURE 10 Requirements for Transcatheter LAA Closure

| WATCHMAN | AMULET | WAVECREST | LARIAT |
|---|--|--|---|
|  |  |  |  |
| <ul style="list-style-type: none"> • The LAA length should be larger than the width (the depth of the main anchoring lobe should be ≥ 19 mm) • Landing zone diameters 17-31 mm • Absence of LAA thrombus | <ul style="list-style-type: none"> • The landing zone is measured 10 mm distally from the ostial plane (the depth of the main anchoring lobe should be >12 mm) • Landing zone diameters 11-31 mm | <ul style="list-style-type: none"> • Required depth of the main anchoring lobe ≤ 10 mm • The landing zone diameters should be 15-29 mm | <ul style="list-style-type: none"> • Ostium diameter should be <40 mm (measured on CT) • Contraindications if: <ul style="list-style-type: none"> • The LAA is oriented superiorly with the apex behind the pulmonary trunk • Multilobed LAA with lobes oriented in different planes exceeding 40 mm • Posteriorly rotated heart • Pericardial disease |

Anatomic characteristics of the left atrial appendage (LAA) for each closure device are summarized. CT = computed tomography.

However, there remain several safety and patient selection concerns that will be addressed in on-going post-marketing surveillance registries and randomized trials (52).

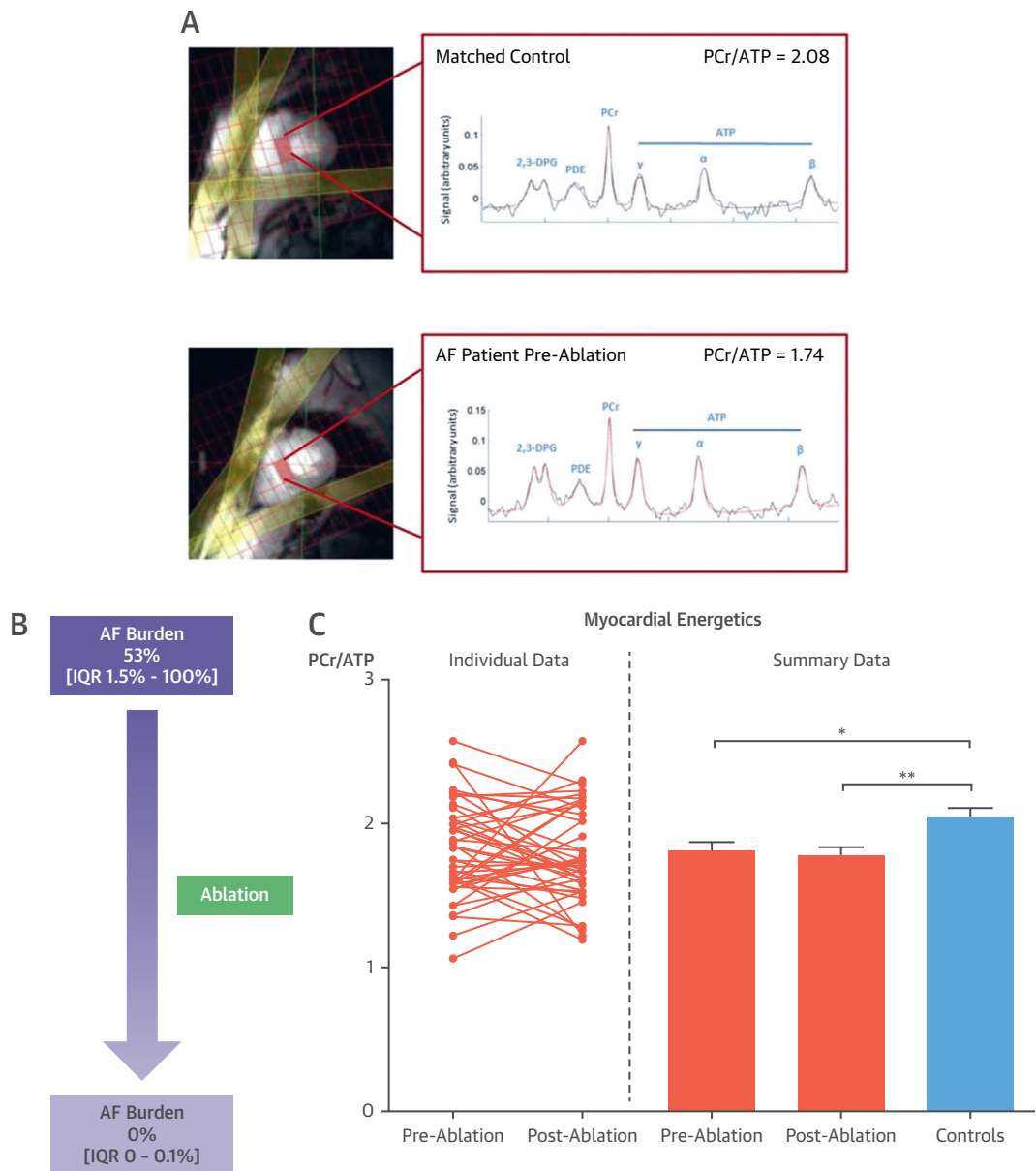
INFLUENCE OF THE LV ON LA REMODELING ASSOCIATED WITH AF

Changes in LV function, structure, and tissue characteristics have also been associated with LA remodeling and AF. However, some uncertainty remains as to the extent to which they are a cause or a consequence of AF (53). CMR techniques have provided new insights into the association of LA remodeling and LV changes in AF. Assessment of diffuse LV myocardial fibrosis with CMR T1-mapping with or without gadolinium-based contrast agents has been applied in patients with AF. Measurement of post-contrast myocardial T1 time allows for accurate measurement of changes in extracellular volume associated with edema or interstitial fibrosis. AF has been associated with higher native (pre-contrast) T1 values (54), lower LV post-contrast T1 values (55), and elevated extracellular volume (56), which are all consistent with the presence of diffuse LV fibrosis. Most importantly, lower LV post-contrast T1 values

have been associated with recurrence of AF after catheter ablation, independent of age and LV systolic dysfunction (55-57). The association between increased LV diffuse fibrosis and LA remodeling was demonstrated by Beinart et al. (58) in 51 patients with AF. Compared with healthy volunteers, AF patients had lower LA and LV post-contrast T1 relaxation times (387 [interquartile range (IQR): 364 to 428] ms vs. 459 [IQR: 418 to 532] ms; $p < 0.001$, and 491 [IQR: 460 to 527] ms vs. 529 [IQR: 496 to 543] ms; $p = 0.074$), respectively. Increasing values of LV post-contrast T1 time correlated modestly with increasing values of LA post-contrast T1 time (Spearman rho correlation coefficient = 0.41; $p < 0.001$), suggesting that myocardial fibrosis affects both the LA and the LV. However, it may be difficult to demonstrate whether LV fibrosis precedes LA fibrosis or vice versa.

In addition, using an index of LV myocardial diffuse fibrosis derived from CMR post-contrast T1 times of the LV, the PRIMERI (Personalized Risk Identification and Management for Arrhythmias and Heart Failure by ECG and CMR) study showed that increasing LV myocardial diffuse fibrosis was associated with electrocardiographic indices of prolonged interatrial conduction in 91 patients in sinus rhythm after adjustment for body mass index,

FIGURE 11 Representative ^{31}P -MRS Spectra and Derived PCr/ATP Ratios From the Mid-Ventricular Septum

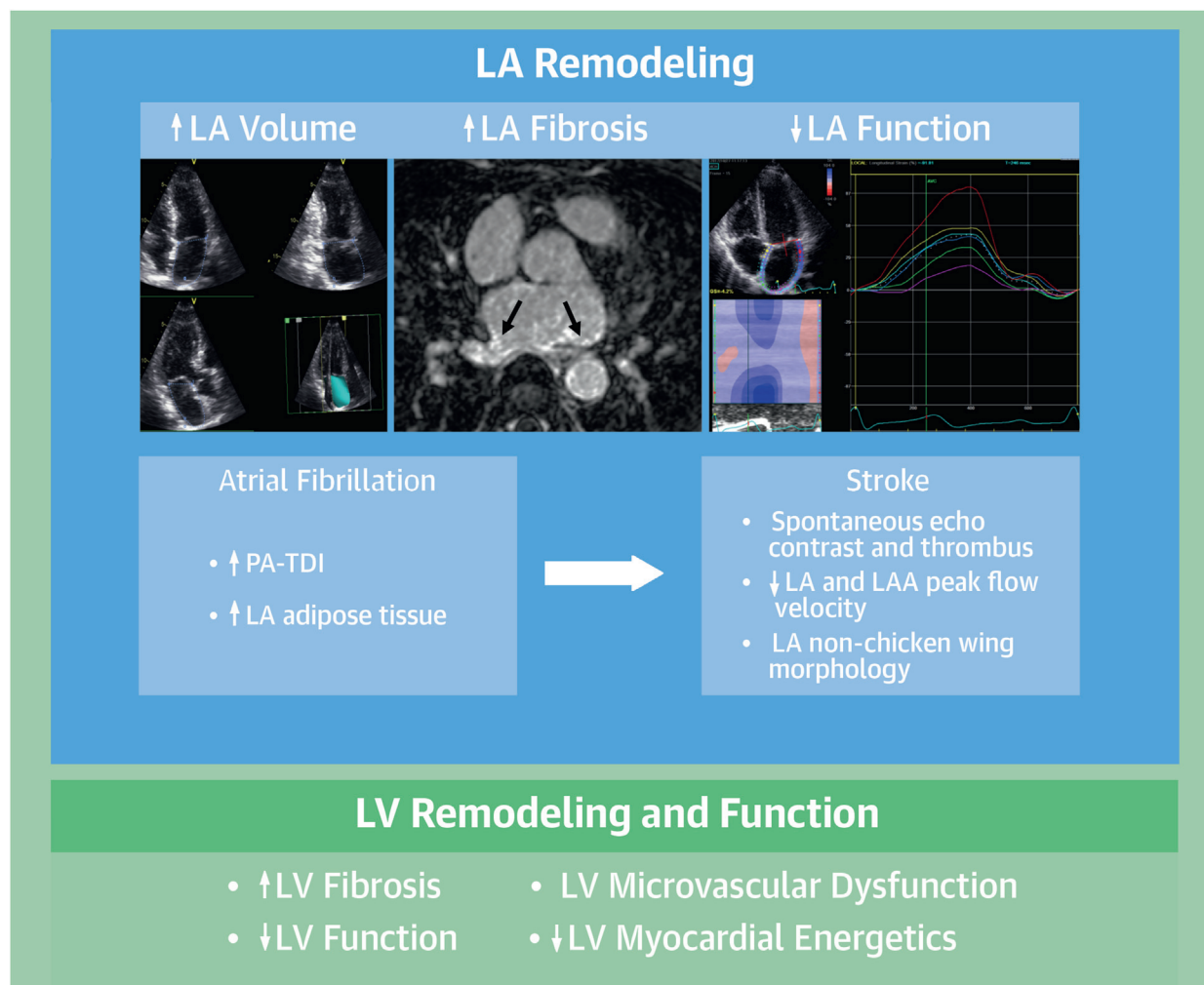


The ^{31}P -MRS spectra and derived PCr/ATP ratios are shown in a matched control subject (**A, top panel**) and an AF patient pre-ablation (**A, bottom panel**). Despite a significant reduction in AF burden at a median of 7 months after catheter ablation ($p < 0.001$) (**B**), there was no change in PCr/ATP ratio in AF patients after ablation ($p = 0.57$) (**C, left panel**), with myocardial energetics remaining significantly impaired compared with matched control subjects in sinus rhythm ($p = 0.001$) (**C, right panel**). Adapted from Wijesurendra et al. (53). 2,3-DPG = 2,3-diphosphoglycerate; ^{31}P -MRS = ^{31}P -magnetic resonance spectroscopy; AF = atrial fibrillation; IQR = interquartile range; PCr/ATP = creatine phosphate/adenosine triphosphate; PDE = phosphodiester.

age, and LV patchy fibrosis detected by LGE (59). Assessment of LV strain with speckle tracking echocardiography permits identification of AF patients with increased LV fibrosis despite showing preserved LV ejection fraction. In 53 AF patients undergoing

radiofrequency catheter ablation, patients who remained in sinus rhythm at follow-up showed better LV longitudinal strain compared with patients who experienced AF recurrences ($-19.6 \pm 2.6\%$ vs. $-17.9 \pm 1.8\%$; $p < 0.005$), whereas no differences were

CENTRAL ILLUSTRATION Association Between LA Remodeling, AF, and Stroke



Delgado, V. et al. *J Am Coll Cardiol.* 2017;70(25):3157–72.

Left atrial (LA) and left atrial appendage (LAA) remodeling are common to the pathophysiology of atrial fibrillation (AF) and stroke. Increased LA volume, increased LA fibrosis, and impaired LA function are the main hallmarks of LA remodeling. Although an increase in LA volume can be assessed with any imaging modality (preferably with 3-dimensional techniques), increased LA fibrosis is evaluated with cardiovascular magnetic resonance (CMR) techniques (**arrows**), and LA function is better assessed with imaging techniques that directly evaluate the myocardial deformation (e.g., speckle tracking echocardiography). Specific imaging parameters related to AF include LA conduction delay, assessed with echocardiographic tissue Doppler imaging (PA-TDI) and increased LA adipose tissue evaluated with computed tomography (CT). Imaging parameters indicating the risk of stroke include blood flow, blood stagnation, and thrombus formation, assessed with transesophageal echocardiography or 4-dimensional flow CMR, and the morphology of the LAA, better assessed with CT. Evaluation of the LA remodeling process underlying the increased risk of atrial fibrillation and stroke should also integrate the influence of the left ventricle (LV), including assessment of LV fibrosis, LV function (strain imaging), microvascular dysfunction (nuclear imaging), and myocardial energetics with magnetic resonance spectroscopy. ↑ = increased; ↓ = reduced.

observed in LV ejection fraction ($59 \pm 7\%$ vs. $61 \pm 6\%$; $p < 0.005$) (60). These findings suggest that changes in atrial tissue characteristics are (partially) the consequence of a global cardiomyopathic process, which plays an important role in promoting the new onset and maintenance of AF, as well as its recurrence after ablation.

Furthermore, LV microvascular dysfunction and altered myocardial energetics may also contribute to the substrate subtending LA remodeling and AF. Patients with AF without obstructive epicardial coronary artery disease have been reported to have significantly reduced LV blood flow measured with $H_2^{15}O$ -positron emission tomography at rest and in

response to adenosine (61). Evidence of LV coronary microvascular dysfunction has also been reported with other techniques in patients with AF (62,63) and in animal models after AF induction (64). Similarly, a reduction in LA perfusion in the presence of AF or following AF induction has been found both in experimental (65,66) and clinical studies (67). Whether coronary microvascular dysfunction has an impact on atrial fibrosis, myocardial energetic status, and cardiac function remains to be established. Nevertheless, LV energetics status evaluated by the phosphocreatine to ATP ratio using 31 phosphorous magnetic resonance spectroscopy is significantly impaired in patients with symptomatic “lone” AF compared with matched control in sinus rhythm and unchanged 7 to 9 months after AF ablation, despite a significant reduction in AF burden and mild improvement in LV ejection fraction (Figure 11) (53). Future studies will need to ascertain the relationship between impaired LV perfusion and energetics on atrial structural and electrophysiological parameters and AF recurrence post-ablation.

CONCLUSIONS

Significant evidence indicates that assessment of LA and LAA anatomy and function has important prognostic implications in new onset and perpetuation of AF and risk of stroke. Selection of patients for anticoagulation treatment or AF ablation does not

routinely include imaging-based parameters that characterize the LA substrate. Anticoagulation therapies are very efficacious in reducing the risk of stroke of AF patients, and LA imaging may not further improve this efficacy in patients at high risk of stroke. Conversely, in patients with low risk of stroke, LA and LAA imaging may further refine the risk and identify patients who may benefit from anticoagulation (enabling “precision medicine”). Importantly, in patients with contraindications for anticoagulation who are referred for transcatheter closure of the LAA, CT and echocardiography play a central role. When selecting patients with AF who may benefit from catheter ablation techniques, imaging techniques to evaluate LA size, function, and myocardial fibrosis have shown to be important. The ongoing DECAAF-II (Efficacy of DE-MRI-Guided Ablation vs. Conventional Catheter Ablation of Atrial Fibrillation II) trial will help to establish the role of LGE CMR to guide ablation procedures and improve the efficacy of the ablation technique. Finally, to understand the LA remodeling process, LV structural and functional changes need to be considered because they are closely interrelated (Central Illustration).

ADDRESS FOR CORRESPONDENCE: Dr. Jeroen J. Bax, Department of Cardiology, Leiden University Medical Center, Albinusdreef 2, 2333 ZA Leiden, the Netherlands. E-mail: j.j.bax@lumc.nl.

REFERENCES

- Benjamin EJ, Blaha MJ, Chiuve SE, et al. Heart Disease and Stroke Statistics-2017 update: a report from the American Heart Association. *Circulation* 2017;135:e146-603.
- Wolf PA, Abbott RD, Kannel WB. Atrial fibrillation as an independent risk factor for stroke: the Framingham Study. *Stroke* 1991;22:983-8.
- Wang TJ, Massaro JM, Levy D, et al. A risk score for predicting stroke or death in individuals with new-onset atrial fibrillation in the community: the Framingham Heart Study. *JAMA* 2003;290:1049-56.
- Pritchett AM, Jacobsen SJ, Mahoney DW, Rodeheffer RJ, Bailey KR, Redfield MM. Left atrial volume as an index of left atrial size: a population-based study. *J Am Coll Cardiol* 2003;41:1036-43.
- Overvad TF, Nielsen PB, Larsen TB, Sogaard P. Left atrial size and risk of stroke in patients in sinus rhythm. A systematic review. *Thromb Haemostasis* 2016;116:206-19.
- Kirchhof P, Benussi S, Kotecha D, et al. 2016 ESC guidelines for the management of atrial fibrillation developed in collaboration with EACTS. *Eur Heart J* 2016;37:2893-962.
- Lang RM, Badano LP, Mor-Avi V, et al. Recommendations for cardiac chamber quantification by echocardiography in adults: an update from the American Society of Echocardiography and the European Association of Cardiovascular Imaging. *J Am Soc Echocardiogr* 2015;28:1-39.
- den Uijl DW, Tops LF, Delgado V, et al. Effect of pulmonary vein anatomy and left atrial dimensions on outcome of circumferential radiofrequency catheter ablation for atrial fibrillation. *Am J Cardiol* 2011;107:243-9.
- Leong DP, Joyce E, Debonnaire P, et al. Left atrial dysfunction in the pathogenesis of cryptogenic stroke: novel insights from speckle-tracking echocardiography. *J Am Soc Echocardiogr* 2017;30:71-9.
- Costa FM, Ferreira AM, Oliveira S, et al. Left atrial volume is more important than the type of atrial fibrillation in predicting the long-term success of catheter ablation. *Int J Cardiol* 2015;184:56-61.
- Oakes RS, Badger TJ, Kholmovski EG, et al. Detection and quantification of left atrial structural remodeling with delayed-enhancement magnetic resonance imaging in patients with atrial fibrillation. *Circulation* 2009;119:1758-67.
- Marrouche NF, Wilber D, Hindricks G, et al. Association of atrial tissue fibrosis identified by delayed enhancement MRI and atrial fibrillation catheter ablation: the DECAAF study. *JAMA* 2014;311:498-506.
- Haemers P, Hamdi H, Guedj K, et al. Atrial fibrillation is associated with the fibrotic remodelling of adipose tissue in the subepicardium of human and sheep atria. *Eur Heart J* 2017;38:53-61.
- Verheule S, Tuyls E, Gharaviri A, et al. Loss of continuity in the thin epicardial layer because of endomyocardial fibrosis increases the complexity of atrial fibrillatory conduction. *Circ Arrhythm Electrophysiol* 2013;6:202-11.
- Abhayaratna WP, Fatema K, Barnes ME, et al. Left atrial reservoir function as a potent marker for first atrial fibrillation or flutter in persons > or = 65 years of age. *Am J Cardiol* 2008;101:1626-9.
- Boyd AC, Schiller NB, Ross DL, Thomas L. Segmental atrial contraction in patients restored to sinus rhythm after cardioversion for chronic atrial fibrillation: a colour Doppler tissue imaging study. *Eur J Echocardiogr* 2008;9:12-7.

17. Schneider C, Malisius R, Krause K, et al. Strain rate imaging for functional quantification of the left atrium: atrial deformation predicts the maintenance of sinus rhythm after catheter ablation of atrial fibrillation. *Eur Heart J* 2008;29:1397-409.
18. Tops LF, Delgado V, Bertini M, et al. Left atrial strain predicts reverse remodeling after catheter ablation for atrial fibrillation. *J Am Coll Cardiol* 2011;57:324-31.
19. De Vos CB, Weijs B, Crijns HJ, et al. Atrial tissue Doppler imaging for prediction of new-onset atrial fibrillation. *Heart* 2009;95:835-40.
20. den Uijl DW, Gawrysiak M, Tops LF, et al. Prognostic value of total atrial conduction time estimated with tissue Doppler imaging to predict the recurrence of atrial fibrillation after radiofrequency catheter ablation. *Europace* 2011;13:1533-40.
21. Tsao HM, Hu WC, Wu MH, et al. Quantitative analysis of quantity and distribution of epicardial adipose tissue surrounding the left atrium in patients with atrial fibrillation and effect of recurrence after ablation. *Am J Cardiol* 2011;107:1498-503.
22. Batal O, Schoenhagen P, Shao M, et al. Left atrial epicardial adiposity and atrial fibrillation. *Circ Arrhythm Electrophysiol* 2010;3:230-6.
23. van Rosendaal AR, Dimitriu-Leen AC, van Rosendaal PJ, et al. Association between posterior left atrial adipose tissue mass and atrial fibrillation. *Circ Arrhythm Electrophysiol* 2017;10:e004614.
24. Benjamin EJ, Blaha MJ, Chiuve SE, et al. Heart disease and stroke statistics-2017 update: a report from the American Heart Association. *Circulation* 2017;135:e146-603.
25. Steinberg BA, Shrader P, Kim S, et al. How well does physician risk assessment predict stroke and bleeding in atrial fibrillation? Results from the Outcomes Registry for Better Informed Treatment of Atrial Fibrillation (ORBIT-AF). *Am Heart J* 2016;181:145-52.
26. van den Ham HA, Klungel OH, Singer DE, Leufkens HG, van Staa TP. Comparative performance of ATRIA, CHADS₂, and CHA₂DS₂-VASc risk scores predicting stroke in patients with atrial fibrillation: results from a national primary care database. *J Am Coll Cardiol* 2015;66:1851-9.
27. Bax JJ, Marsan NA, Delgado V. Non-invasive imaging in atrial fibrillation: focus on prognosis and catheter ablation. *Heart* 2015;101:94-100.
28. Atrial Fibrillation Investigators. Echocardiographic predictors of stroke in patients with atrial fibrillation: a prospective study of 1066 patients from 3 clinical trials. *Arch Intern Med* 1998;158:1316-20.
29. Di Biase L, Santangeli P, Anselmino M, et al. Does the left atrial appendage morphology correlate with the risk of stroke in patients with atrial fibrillation? Results from a multicenter study. *J Am Coll Cardiol* 2012;60:531-8.
30. Zabalgoitia M, Halperin JL, Pearce LA, Blackshear JL, Asinger RW, Hart RG. Stroke Prevention in Atrial Fibrillation III Investigators. Transesophageal echocardiographic correlates of clinical risk of thromboembolism in nonvalvular atrial fibrillation. *J Am Coll Cardiol* 1998;31:1622-6.
31. Inoue YY, Alissa A, Khurram IM, et al. Quantitative tissue-tracking cardiac magnetic resonance (CMR) of left atrial deformation and the risk of stroke in patients with atrial fibrillation. *J Am Heart Assoc* 2015;4:e001844.
32. Akoum N, Fernandez G, Wilson B, McGann C, Kholmovski E, Marrouche N. Association of atrial fibrosis quantified using LGE-MRI with atrial appendage thrombus and spontaneous contrast on transesophageal echocardiography in patients with atrial fibrillation. *J Cardiovasc Electrophysiol* 2013;24:1104-9.
33. Daccarett M, Badger TJ, Akoum N, et al. Association of left atrial fibrosis detected by delayed-enhancement magnetic resonance imaging and the risk of stroke in patients with atrial fibrillation. *J Am Coll Cardiol* 2011;57:831-8.
34. Lee DC, Markl M, Ng J, et al. Three-dimensional left atrial blood flow characteristics in patients with atrial fibrillation assessed by 4D flow CMR. *Eur Heart J Cardiovasc Imaging* 2016;17:1259-68.
35. Blackshear JL, Odell JA. Appendage obliteration to reduce stroke in cardiac surgical patients with atrial fibrillation. *Ann Thorac Surg* 1996;61:755-9.
36. Wang Y, Di Biase L, Horton RP, Nguyen T, Morhanty P, Natale A. Left atrial appendage studied by computed tomography to help planning for appendage closure device placement. *J Cardiovasc Electrophysiol* 2010;21:973-82.
37. Ismail TF, Panikker S, Markides V, et al. CT imaging for left atrial appendage closure: a review and pictorial essay. *J Cardiovasc Comput Tomogr* 2015;9:89-102.
38. Yaghi S, Song C, Gray WA, Furie KL, Elkind MS, Kamel H. Left atrial appendage function and stroke risk. *Stroke* 2015;46:3554-9.
39. Davis CA 3rd, Rembert JC, Greenfield JC Jr. Compliance of left atrium with and without left atrium appendage. *Am J Physiol* 1990;259:H1006-8.
40. Chapeau C, Gutkowska J, Schiller PW, et al. Localization of immunoreactive synthetic atrial natriuretic factor (ANF) in the heart of various animal species. *J Histochem Cytochem* 1985;33:541-50.
41. Di Biase L, Burkhardt JD, Mohanty P, et al. Left atrial appendage: an underrecognized trigger site of atrial fibrillation. *Circulation* 2010;122:109-18.
42. Di Biase L, Burkhardt JD, Mohanty P, et al. Left atrial appendage isolation in patients with long-standing persistent AF undergoing catheter ablation: BELIEF trial. *J Am Coll Cardiol* 2016;68:1929-40.
43. Manning WJ, Weintraub RM, Waksmonski CA, et al. Accuracy of transesophageal echocardiography for identifying left atrial thrombi. A prospective, intraoperative study. *Ann Intern Med* 1995;123:817-22.
44. The Stroke Prevention in Atrial Fibrillation Investigators. Predictors of thromboembolism in atrial fibrillation: II. Echocardiographic features of patients at risk. *Ann Intern Med* 1992;116:6-12.
45. Burrell LD, Horne BD, Anderson JL, Muhlestein JB, Whisenant BK. Usefulness of left atrial appendage volume as a predictor of embolic stroke in patients with atrial fibrillation. *Am J Cardiol* 2013;112:1148-52.
46. Jung PH, Mueller M, Schuhmann C, et al. Contrast enhanced transesophageal echocardiography in patients with atrial fibrillation referred to electrical cardioversion improves atrial thrombus detection and may reduce associated thromboembolic events. *Cardiovasc Ultrasound* 2013;11:1.
47. Fatkin D, Kelly RP, Feneley MP. Relations between left atrial appendage blood flow velocity, spontaneous echocardiographic contrast and thromboembolic risk in vivo. *J Am Coll Cardiol* 1994;23:961-9.
48. Lupercio F, Carlos Ruiz J, Briceno DF, et al. Left atrial appendage morphology assessment for risk stratification of embolic stroke in patients with atrial fibrillation: a meta-analysis. *Heart Rhythm* 2016;13:1402-9.
49. Hur J, Kim YJ, Lee HJ, et al. Cardioembolic stroke: dual-energy cardiac CT for differentiation of left atrial appendage thrombus and circulatory stasis. *Radiology* 2012;263:688-95.
50. Teunissen C, Habets J, Velthuis BK, Cramer MJ, Loh P. Double-contrast, single-phase computed tomography angiography for ruling out left atrial appendage thrombus prior to atrial fibrillation ablation. *Int J Cardiovasc Imaging* 2017;33:121-8.
51. Romero J, Husain SA, Kelesidis I, Sanz J, Medina HM, Garcia MJ. Detection of left atrial appendage thrombus by cardiac computed tomography in patients with atrial fibrillation: a meta-analysis. *Circ Cardiovasc Imaging* 2013;6:185-94.
52. Piccini JP, Sievert H, Patel MR. Left atrial appendage occlusion: rationale, evidence, devices, and patient selection. *Eur Heart J* 2017;38:869-76.
53. Wijesurendra RS, Liu A, Eichhorn C, et al. Lone atrial fibrillation is associated with impaired left ventricular energetics that persists despite successful catheter ablation. *Circulation* 2016;134:1068-81.
54. Kato S, Foppa M, Roujol S, et al. Left ventricular native T1 time and the risk of atrial fibrillation recurrence after pulmonary vein isolation in patients with paroxysmal atrial fibrillation. *Int J Cardiol* 2016;203:848-54.
55. Ling LH, Kistler PM, Ellims AH, et al. Diffuse ventricular fibrosis in atrial fibrillation: noninvasive evaluation and relationships with aging and systolic dysfunction. *J Am Coll Cardiol* 2012;60:2402-8.
56. Neilan TG, Mongeon FP, Shah RV, et al. Myocardial extracellular volume expansion and the risk of recurrent atrial fibrillation after pulmonary vein isolation. *J Am Coll Cardiol Img* 2014;7:1-11.

57. McLellan AJ, Ling LH, Azzopardi S, et al. Diffuse ventricular fibrosis measured by T(1) mapping on cardiac MRI predicts success of catheter ablation for atrial fibrillation. *Circ Arrhythm Electrophysiol* 2014;7:834-40.
58. Beinart R, Khurram IM, Liu S, et al. Cardiac magnetic resonance T1 mapping of left atrial myocardium. *Heart Rhythm* 2013;10:1325-31.
59. Tiffany Win T, Ambale Venkatesh B, Volpe GJ, et al. Associations of electrocardiographic P-wave characteristics with left atrial function, and diffuse left ventricular fibrosis defined by cardiac magnetic resonance: the PRIMERI study. *Heart Rhythm* 2015;12:155-62.
60. Tops LF, den Uijl DW, Delgado V, et al. Long-term improvement in left ventricular strain after successful catheter ablation for atrial fibrillation in patients with preserved left ventricular systolic function. *Circ Arrhythm Electrophysiol* 2009;2:249-57.
61. Range FT, Schafers M, Acil T, et al. Impaired myocardial perfusion and perfusion reserve associated with increased coronary resistance in persistent idiopathic atrial fibrillation. *Eur Heart J* 2007;28:2223-30.
62. Luo C, Wu X, Huang Z, et al. Documentation of impaired coronary blood flow by TIMI frame count method in patients with atrial fibrillation. *Int J Cardiol* 2013;167:1176-80.
63. Smit MD, Tio RA, Slart RH, Zijlstra F, Van Gelder IC. Myocardial perfusion imaging does not adequately assess the risk of coronary artery disease in patients with atrial fibrillation. *Europace* 2010;12:643-8.
64. Bukowska A, Hammwöhner M, Sixdorf A, et al. Dronedron prevents microcirculatory abnormalities in the left ventricle during atrial tachypacing in pigs. *Br J Pharmacol* 2012;166:964-80.
65. van Bragt KA, Nasrallah HM, Kuiper M, Luiken JJ, Schotten U, Verheule S. Atrial supply-demand balance in healthy adult pigs: coronary blood flow, oxygen extraction, and lactate production during acute atrial fibrillation. *Cardiovasc Res* 2014;101:9-19.
66. White CW, Holida MD, Marcus ML. Effects of acute atrial fibrillation on the vasodilator reserve of the canine atrium. *Cardiovasc Res* 1986;20:683-9.
67. Skolidis EI, Hamilos MI, Karalis IK, Chlouverakis G, Kochiadakis GE, Vardas PE. Isolated atrial microvascular dysfunction in patients with lone recurrent atrial fibrillation. *J Am Coll Cardiol* 2008;51:2053-7.

KEY WORDS atrial fibrillation, left atrial appendage, left atrium, multimodality imaging, stroke